ISSN 2347-3487
Journal of Advances in Physics

Influence of rapid solidification and lithium additions on microstructure and mechanical properties of aluminum based alloys

Rizk Mostafa Shalaby[1,*], Mustafa Kama1[1] and Adel. S. Waqlan[1, 2]
[1]Metal Physics Laboratory, Physics Department, Faculty of Science, Mansoura University, Mansoura, Egypt, P.O.Box:35516.
[2] Physics department, Faculty of Science and Education, Amran University, Yamen
* Email: rizk 2002@mans.edu.eg, doctorrizk2@yahoo.co.uk
Adel.S.waqlan@gmail.com

Abstract

A series of aluminum-lithium or lightweight alloys containing up to 5 wt. % lithium was rapidly solidified from melt by melt-spinning method. The prepared ribbons were scanned via scanning electron microscope (SEM), X-ray diffraction (XRD) and deferential scanning calorimetry (DSC) techniques. The results showed that the structures of all melt- spinning ribbons were completely composed of two distinct phases' aluminum rich phase and intermetallic compound (IMC) Al9.8-Li1.1phase. It's also observed with increasing of lithium content the melting point, solidus and liquidus temperatures was slightly decreased. as well as internal friction, elastic moduli, hardness and thermal diffusivity measurements of melt-spun ribbons was studied via utilizing dynamic resonance method and Vickers hardness for one applied load of 25 grams-force for 5.0, 20.0, 40.0, 60.0, 80.0 and 99.0 second. We observed Aluminum rich phase is finer in intermetallic compound and grain size, after the adding of Lithium, is more uniformly distributed. As a result, Young's modulus and micro-hardness of Lightweight are increased when Lithium was added into the Aluminum alloy. The aim of the research planned in this work was to design the A1-Li family of alloys contribute to their increasingly broad applications in Aerospace, as an alternative for the aluminum alloys, which have been used so far.

Keywords: Rapid solidification; Al-Li alloys; microstructure; thermal properties; mechanical properties

1. Introduction

Lightweight alloys represent a class of high performance is related to the fact that the Li content decreases the density and increases the Young modulus. The most attractive reason for alloying with Li is the beneficial impact on stiffness and weight reduction. from the early 1920s, aluminum alloys have been the primary material in the aircraft industry, due to a combination of properties including low density, corrosion resistance, ductility, stiffness and specific strength [1,2]. The Al–Li alloys have attractive applications in the aerospace industry due to their lower density, better strength and high stiffness comparing to the conventionally commercial and series aluminum alloys[3]. Li is the lightest metallic element, with a density of 0.54 g/cm^3; it has a high solid solubility in aluminum, with a maximum of approximately 4.2% wt. at 610°C. Each 1 wt.% lithium added to the Al-Li alloy lead to 3% reducing in its density and increased the elastic modulus by about 6%[4–6]. The mechanical properties of the high-strength Al-Li alloys, as compared to those of the conventional ones, can be increased by a few wt.%. Moreover, lithium has an especially good impact on the improvement of the crack resistance, the fatigue resistance add to the effect resistance at low temperatures. Lithium has a high solubility in aluminum amount to 14 at. % at 600°C, which reduced together with temperature, and this create a possibility to model the mechanical properties using of heat treatment[7]. In the AlLi phase equilibrium system as shown Fig.1 the following phases are present: a solution of lithium in Aluminum, with the RSC structure, an intermetallic phase, δ, based on the AlLi compound with a variable solubility in lithium in the range from about 45 to 55% at; intermetallic compounds:Al4Li3, stable up to520°C, and Al4Li9, stable up to 330°C[8]. This offers a weight savings that would be extremely valuable for many applications, especially the aerospace industry. The present research and development of aluminum-lithium alloys is being driven by the requirement for the aluminum industry to improve their present alloys. As new advanced composites challenge the dominance of aluminum for used in aircraft production, the aluminum industry must be develop best alloys to stay competitive. Add of the lithium for an alloying aluminum since long, Attributed to the reduction in density and increase in strength add to some deleterious properties such as a decrease in toughness and ductility. These problems has niggle the development of Al-Li alloys. Present, there are now available some aluminum alloys that do have lithium mixed into them. However, these present alloys are not capable of universally replace all applications of conventional alloys. These alloys also are mixed with two or more addition element, thus reduction the major advantage of lithium addition [9]. The Improvement of the fracture tolerance, strength

properties and decrease mechanical property anisotropy of Al–Li alloy is request to be convenient for operating in next generation. However, there is as yet an interest in developed the next generation of Al–Li alloy with improvement specific strength, damage tolerance and reduced mechanical property anisotropy[10]. Aluminum-Lithium alloys enhancement stiffness and density due to the lithium addition to the aluminum. The Li is one element which has substantial solubility in solid Al (4.20 wt. % in binary Al-Li alloys). The probability for alloys density of aluminum decrease within addition of lithium is clear via comparison its atomic weight (6.940) with that of aluminum (26.980). Commercial importance of Al-Li Alloys is derived from the fact that a great numbers of examinations carried out in USA, France and UK within 10-15 last year's[5]. The properties of the high-strength Al-Li alloys depend on the microstructure, fundamentally on the size, morphology of the grains. The microstructure characteristics which significantly impact the mechanical properties of the alloy are: the type and size of the precipitate, their distribution in the matrix as well as their coherence with the matrix[11]. Rioja RJ et al[12] reported that the Aluminum-Lithium alloys contain higher than 2 wt.% Lithium has significantly decrease anisotropic properties compare to those present obtainable, then a new Aluminum-Lithium alloy C489 by optimization of composition chemical and processing method was advanced. but, the elongation of the alloy at high temperature conditions was applied in aircrafts industry while higher elongation for the same alloy which due to similar isotropic mechanical properties at medium temperature have been occurred [13].The elastic properties of aluminum alloys were affected by behavior of Li additions in the alloy matrix or present as second phase or as solution [14].

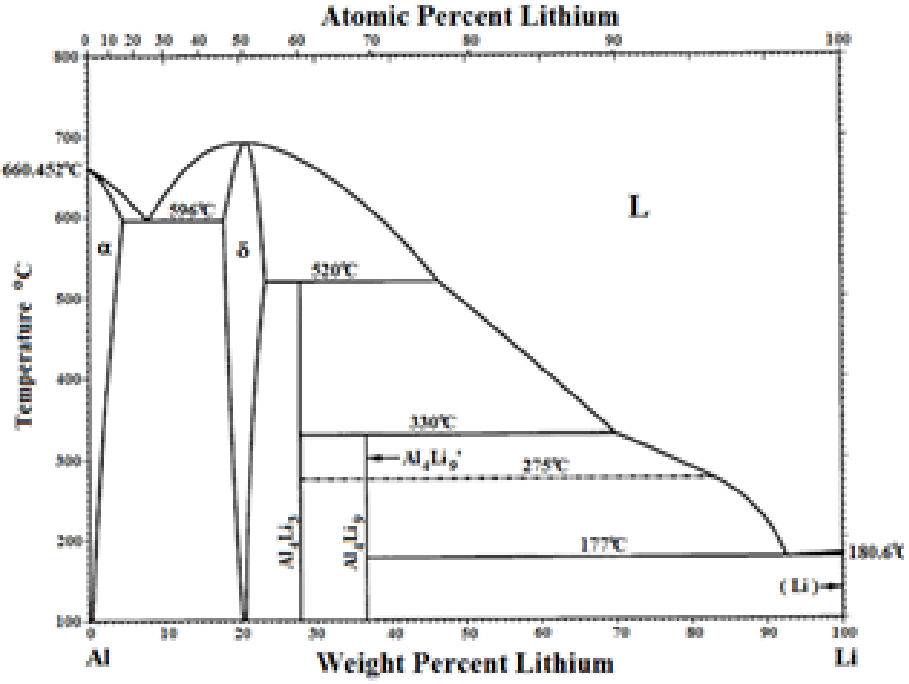

Fig.1: Phase equilibrium diagram of Al-Li[8].

2. Experimental procedures

Were prepared six alloys of compositions Al pure, Al-1Li%, Al-2LI%, Al-3Li%, Al-4Li% and Al-5Li%, in form ribbons from rang 0.40-0.50cm width and has thickness about rang 0.014-0.020 cm. was prepared via a single copper roller melt-spinning method [15]. If we supposed that the ribbons became completely solid at a distance, d, from point of impinge of the molten current, the solidification average R was calculated via:

$$R = \frac{t.v}{d} \dots\dots\dots\dots\dots\dots\dots\dots\dots\dots (1)$$

Where v is the surface speed of the wheel and t is the ribbon's thickness, therefore the solidification average R is the range 10^{-5}-10^{-4} m/s. hence solid ribbons can be observed leave the surface wheel after nearly a tenth of one revolution where $d \approx 0.5$cm[16]. The materials used in the present work are aluminum and Lithium as granules, and the starting purity was than 99.99 %. A group of AL-Li_X (where x=1, 2, 3, 4, and 5 in wt. %), weighted and melted down in the porcelain crucible at melt temperature of 750◦C. The operation parameters such as, the linear speed and the expulsion temperature of the copper wheel were fixed at 30.4 m/s and 550k respectively. The flow rate experimentally found to be an important melt-spun process changing and its dependent on easily adjustable device parameters which reported by Liebermann. [17]. This parameter is calculated by:

$$Q_f = V_r W t \ldots\ldots\ldots\ldots\ldots\ldots\ldots\ldots\ldots\ldots (2)$$

Where (W) is the ribbon width, (Vr) is the ribbon or substrate speed and (t) the average thickness calculated by:

$$t = \frac{m}{lw\rho} \ldots\ldots\ldots\ldots\ldots\ldots\ldots\ldots\ldots\ldots (3)$$

Where (l) is the ribbon length, (ρ) is the density and (m) is the mass. X-ray diffraction examination was completed on a Shimadzu (x-ray diffractmeter -30), utilizing Cu kα radiation (λ=1.5406 Å) with Ni-refinery. The microstructure examining was carried out on a scanning electron microscope of kind JSM-6510 LV JEOL (Japan), operating at (30 kV) resolution in high vacuum mode, and 3.0 nm. Differential scanning calorimetry of type SDT Q600, USA , 10^{o}C/min .The Vickers microhardness tester of type FM-7, Japan, applying a load of 25 gram force for 5.0,20.0,40.0,60.0,80.0 and 99.0 a second, by a diamond pyramid[18].

3. Results and Discussions

3.1 Structure

3.1.1 X-ray examinations

metal alloys prepared using Rapid solidified from melt was reported by Pol Duwez et al [19].The X-ray diffraction (XRD) patterns of the melt-spun AL-Li$_x$ (where X=1,2,3,4 and 5wt. %) ribbons rapid solidified from melt at (750 ^{o}C). The X-ray analysis of the AL-Li alloy shows the phases of structure, face centered cubic α-Al and intermetallic compounds AlLi[20]. From X-ray diffraction patterns of Al-Lix (x= 1, 2, 3, 4, 5 wt. %) alloy as indicates show that two phases of the structure face centered cubic α-Al and intermetallic compounds Al8.9Li1.1 at 2θ=38.506^o,44.761^o,65.158^o,78.308^o,82.521^{o}and 99.194^o of alloys as shown in Fig.2. From x-ray analysis, adding Li content to Al alloy produced a change in its matrix microstructure (particle size, unit cell volume, lattice parameters and lattice distortion) and the shape of formed phases such as peak intensity, peak broadness and peak position. Through X-ray diffraction get micro strain right with lithium addition to 4w% and an increase in intensity that is Attributed to lithium atoms melt in Al matrix formed a solidsolution\or some Li atoms formed a trace of undetected phases (α-Al or Al8.9Li1.1 intermetallic phases), also a clear increase particle size to 4w%. This increase in particle size due to reduce in the grain boundaries, due to enhanced in mechanical properties. Also, the studied lattice parameters, (a=b=c), crystal size, lattice distortion and unit volume cell of face centered cubic α-Al phase in Al-Li$_x$ (x= 1, 2, 3, 4, 5 wt. %) alloys are listed in Table.1. To get this number me use the reality that volume of the unit cell, calculated through the lattice parameters by using equations these give the volume V with the unit cell.

Cubic $V = a^3$ ……..... (4)

So, from the following equation

$$\rho = \frac{1.66020 \Sigma A}{V} \ldots\ldots\ldots\ldots\ldots\ldots\ldots\ldots (5)$$

We have

$$\Sigma A = \frac{\rho V}{1.660202} \ldots\ldots\ldots\ldots\ldots\ldots\ldots\ldots\ldots\ldots . (6)$$

Where V is the volume of the unit cell, ρ is the density gm/cm^3 and (ΣA) is the sum of the atomic weights of the atoms in the unit cell. We can calculate number of atoms per cell from n, where ΣA= n A, and A is the Molecular mass. To determine information about the local lattice deformation and crystallite size (D$_{eff}$) in α-Al phases by the next formula [21] :

$$B = \frac{1}{D_{eff}} + 5 <\Sigma^2>^{\frac{1}{2}} \frac{Sin\theta}{\lambda} \ldots\ldots (7)$$

The $1/D_{eff}$ and $5 < \varepsilon^2 >^{½}$ are given in Table.1.

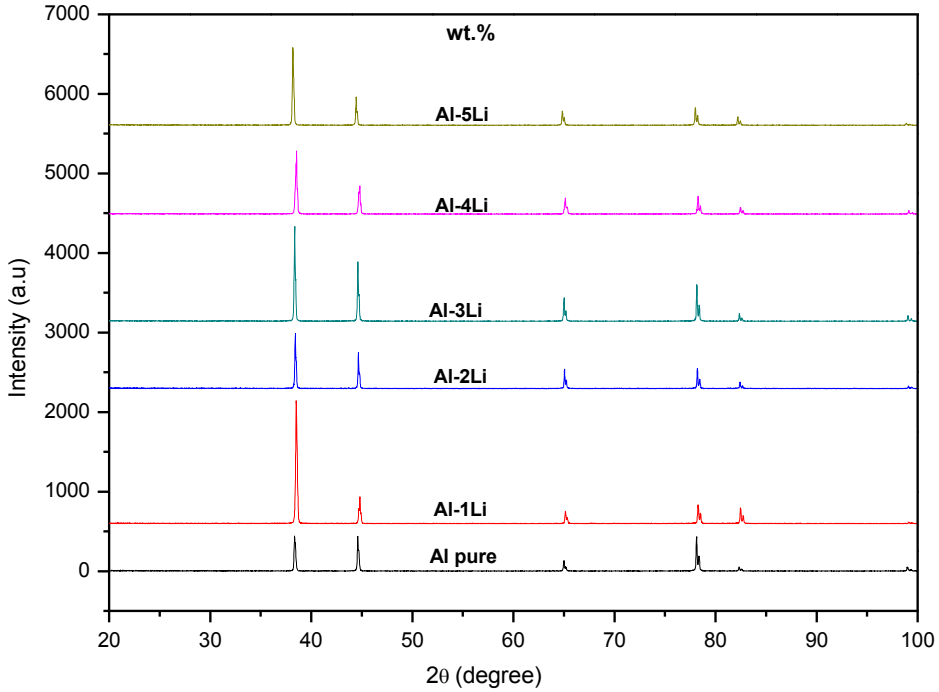

Fig.2. The XRD patterns of melt-spun ribbons.

Table 1: Number of atoms per unit cell, unit cell volume, lattice parameters, particle size and lattice distortion of melt spun alloys system.

Composition wt.% as melt spun Ribbons	a (A^0)	Cell volume(A^o)^3	Number of atoms/unit cell	Particle size (A^o)	1/Deff (A^{o-1})	$5 < \Sigma^2 >^{1/2}$
Al pour	4.0582	66.836	4.02876	405.775	0.00170	0.0035
Al-1Li	4.04717	66.2910	2.10699	409.581	0.00164	0.0034
Al-2Li	4.0524	66.5491	1.774	458.070	0.001431	0.0029
Al-3Li	4.0563	66.742	1.722	446.686	0.00145	0.0030
Al-4Li	4.04729	66.2972	1.897	428.192	0.00167	0.0034
Al-5Li	4.0666	67.251	2.16887	405.491	0.00160	0.0033

3.1.2 Microstructure

The Scanning electron microscope (SEM) micrograph clarify the existence of scattered particles in the Al matrix, as appeared in Fig.3. It display an exemplary (SEM) micrograph of the melt-spinning ribbons of (light) Revealed a found scattering of the lithium particles in the aluminum matrix (dark). The Change in Li content have a marked effect on the solidification mechanism as displays from through microstructure when content the Higher than 4 wt. % Lithium. The increase the particle size, because decreased grain boundaries and increasing the mechanical properties as shown by X-ray calculations. It can be seen that the microstructures of Prepared alloys by of the melt-spun rapid solidification Copper wheel lower coarser. This is probably due to the fact that the cooling of the Copper wheel is higher than that any technique .The microstructural variation at different addition was observed by SEM as shown in Fig.3.

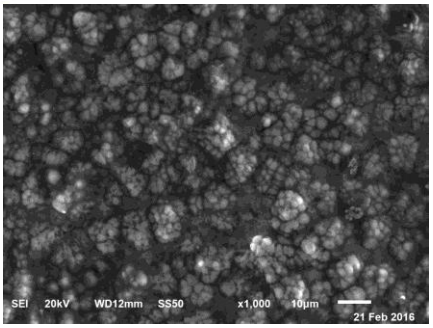

Al pure (a)

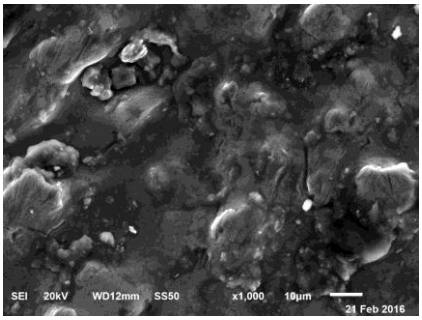

Al-1Li wt.% (b)

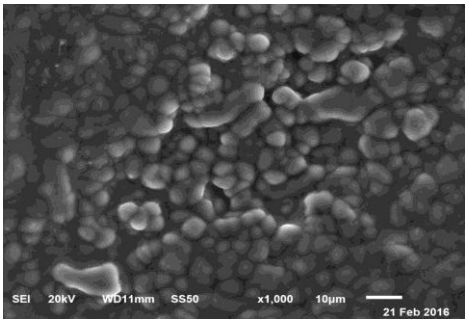

Al-2Li wt.% (c)

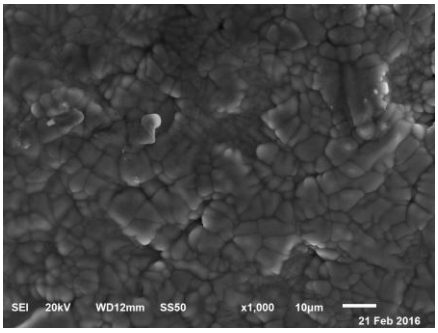

Al-3Li wt.% (d)

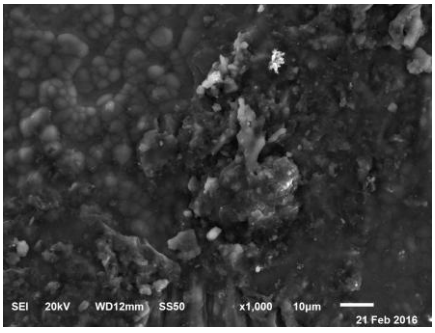

Al-4Li wt.% (e)

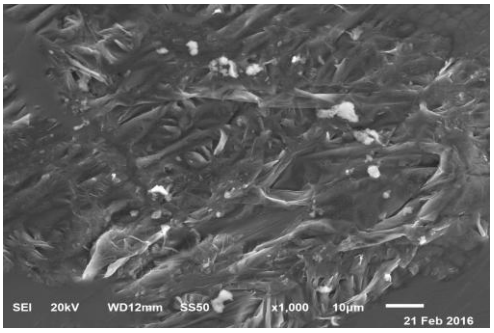

Al-5Li wt.% (f)

Fig.3: SEM micrograph of melt-spun ribbons (a, b.c.d, e and f) alloys.

4. Thermal properties

The quantities of thermal properties depend on the nature of solid phase and on its temperature. The differential scanning calorimeter (DSC) thermo-graphs were achieved with heat rate $10^{o}C\ min^{-1}$ at the temperature range from 0.0- $800^{o}C$. Fig.4, displays the deferential scanning calorimetry (DSC) curve of rapidly solidified of Al and Al-Li_x (x= 1, 2, 3, 4 and 5 wt. %) alloys. one endo-thermic peak was observed in the rapidly solidified alloy, sited at 663.41,664.19,662.88,663.9,663.4 and 663.5, respectively. The endo-thermic peak corresponds to the melting point of rapidly solidified of Al and Al-Lix (x= 1, 2, 3, 4 and 5 wt. %) alloys. From these graphs the liquidus temperature(T_L), melting point (T_m) and solidus temperature (T_s), other thermal parameters (entropy, ΔS, enthalpy, ΔH, and specific heat, C_p) of Al-Li_x (where x= 1, 2, 3, 4 and 5 wt. %) alloys are identified and then listed in Table.2. A little variation occurred in thermo-graph (Endo-thermal peaks) of Al-Li alloy after adding Lithium. That is Attributed to Li atoms solve in aluminum matrix due to variance its structure which correspond with x-ray examined. The melting temperature of Al-Li slightly changes with adding Li content. Also, enthalpy, ΔH, Specific heat, C_p and other thermal parameters of Al-Li alloy varied after adding Lithium content.

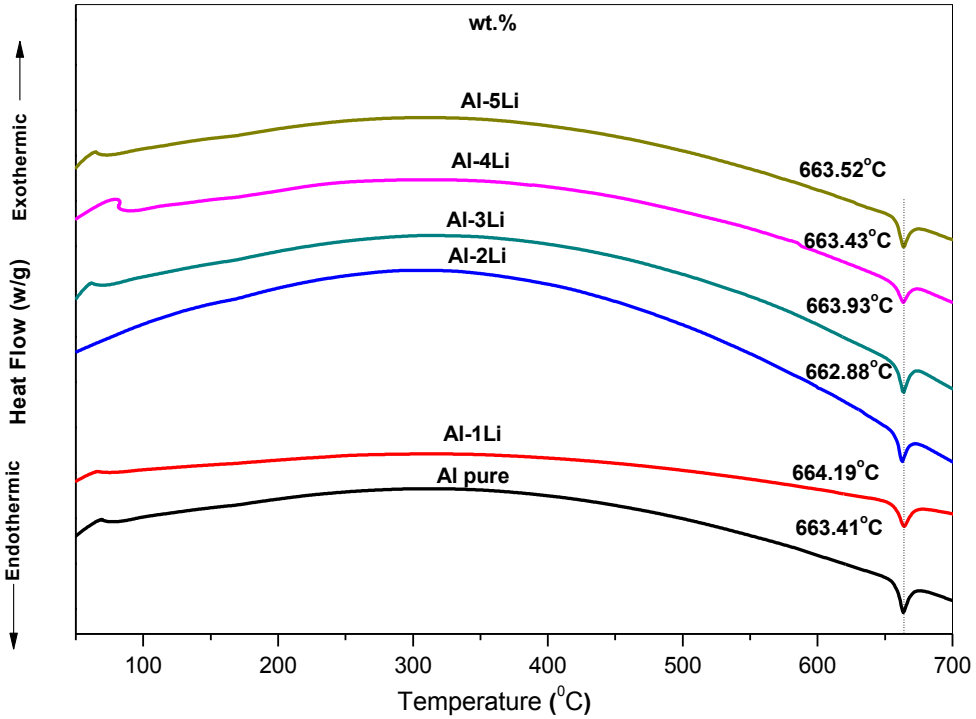

Fig .4: DSC graphs of melt-spun ribbons.

Table 2: Thermal analysis of melt spun alloys system.

Composition wt.% as melt spun Ribbons	Tm (K)	Ts (K)	T_L (K)	Enthalpy ΔH (j/g)	heat of Specific Cp (j/g. k)	change of Entropy ΔS (j/g. k)
Al pure	936.41	931.37	953.22	1296	59.313	1375.674
Al-1Li	937.19	931.24	951.62	1101	54.023	1169.753
Al-2Li	935.88	931.63	949.32	903	51.045	960.354
Al-3Li	936.93	931.27	952.064	1166	56.073	1238.503
Al-4Li	936.43	930.31	952.06	846.4	38.914	899.493
Al-5Li	936.52	931.65	947.87	987.5	60.881	1051.015

5. Mechanical properties

5.1 Internal friction, thermal diffusivity and Young's modulus

There are advantage of dynamic resonance process over static method to measure modulus of elastic due to low level stress not bloat an elastic method for example elastic hysteresis or creep[22,23]. From resonance method with elastic moduli was obtained of information of elastic compliances within the long axis in melt – spun ribbons. Can be obtained of elastic moduli from frequency f_o, where peak damping occurs, depending on:

$$E = \frac{38.32\rho l^4 f^2}{t^2} \quad \ldots\ldots\ldots\ldots\ldots\ldots (8)$$

$$G = \frac{E}{2(1+v)} \quad \ldots\ldots\ldots\ldots\ldots\ldots\ldots (9)$$

$$B = \frac{E}{3(1-2v)} \ldots\ldots\ldots\ldots\ldots\ldots\ldots (10)$$

Where, ρ is ribbon density, *l* is vibrated part of ribbon, *E* is young's modulus, *t* is ribbon thickness, *B* is bulk modulus, *G* is share modulus and *v* is poison's ratio. Internal friction measurement is one of sensitive ways that are suitable to examination microstructural changes and defect motion, such as atomic diffusion, dislocation activity and grain boundary sliding. The internal friction Q^{-1} values which calculated from resonance peak shows in fig .5. These one of characteristics of important are indirect related to their properties of elastic. The free vibration is determined by the decay of measurement in amplitude of vibrations during free vibration. The internal friction can be calculated by [24]:

$$Q^{-1} = 0.5773\frac{\Delta f}{f_0} \ldots\ldots\ldots\ldots\ldots\ldots (11)$$

The effect of the bulk stiffness's and shear on Poisson's ratio can be calculated through the relationship:

$$v = \frac{1}{2}\left[\frac{(3B/G)-2}{(3B/G)+1}\right] \qquad (12),$$

The value of increase of Young's modulus with addition Li, might because by microstructure observations revealed the presence of high density precipitates of intermetallic phases, both inside the grains and at the grain limits and Large particles of intermetallic phases have significant effect on Young's modulus. The Values of bulk modulus *B*, shear modulus *G*, young modulus *E*, Poisson's ratio, and internal friction result of Al and Al-Li_x (where x=1,2,3,4 and 5 wt.) alloys rapidly solidified from melt–spun ribbons listed in table.3.

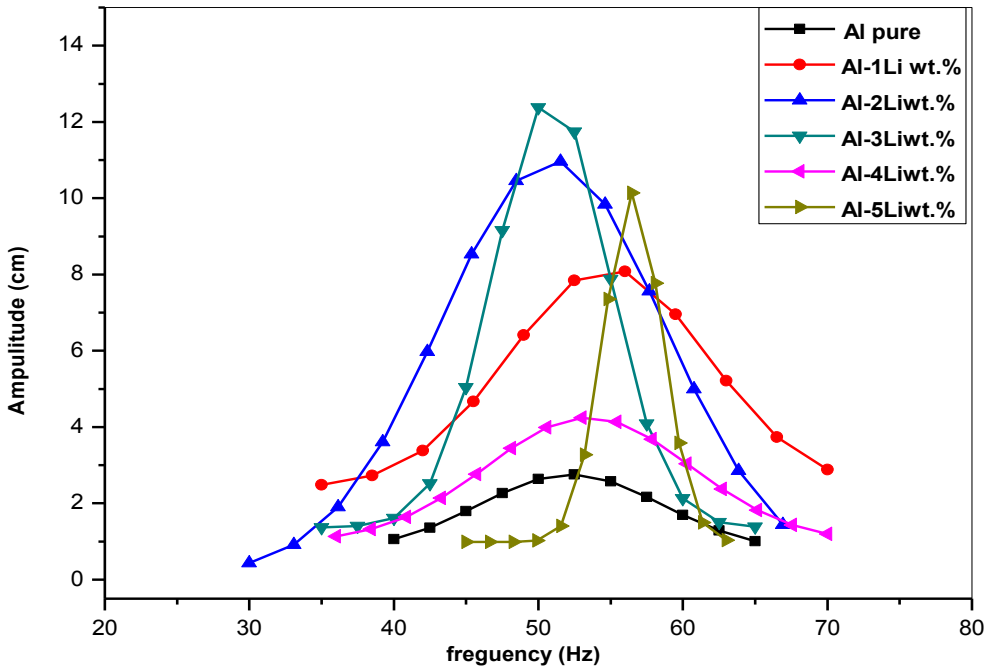

Fig .5: Resonance curves of melt-spun ribbons

Table 3: Mechanical properties of melt– spun alloys system.

Composition wt.% as melt spun Ribbons	Young's modulus (*E*) GPa	Bulk modulus (*B*) GPa	Shear modulus (*G*) GPa	Internal frication Q^{-1} (10^{-3})	Poisson's ratio
Al pure	67	75	25	60	0.35
Al-1Li	75	84	28	46	0.351

Al-2Li	77	87	29	34	0.353
Al-3Li	64	73	24	30	0.354
Al-4Li	79	91	30	19	0.356
Al-5Li	95	110	35	23	0.357

The time rate of temperature change Determines the values thermal diffusivity of any a material when heat via through material as showed in the table .4. Can be calculated thermal diffusivity From the reverberation frequency f_o, at which the top damping occurs utilizing the dynamic reverberation method utilizing equation [25,26].

$$D_{th} = \frac{2d^2 f_o}{\pi} \quad \ldots\ldots\ldots\ldots\ldots\ldots (13)$$

Where d is the thickness of ribbon. For Al and Al-Lix (where x=1, 2, 3, 4 and 5 wt. %), melt–spun alloys, the thermal diffusivity is higher than Al-1Li from Al pure and Al-Lix (where x=2, 3, 4 and 5 wt. %) alloys. But in the case of Al-2Li alloys, there are a slightly decrease of thermal diffusivity. This is may be due to segregation of Al8.9-Li1.1nanoparticles as indicated in the x-ray diffraction examination.

Table 4: Thermal Diffusivity of melt spun alloys system.

Composition wt.% as melt spun Ribbons	Thermal Diffusivity $D_{th}\,10^{-3}$ (cm^2/sec)
AL pure	11.8
Al-1Li	13.3
Al-2Li	9.5
Al-3Li	10.4
Al-4Li	11.1
Al-5Li	11.7

5.2 Microhardness and microcreep

The properties of mechanical of Al pure and Al-Lix (where x=1, 2, 3, 4 and 5 wt. %), melt–spun alloys can be determined by Vickers micohardness utilizing the standard Vickers formula, depending on literature of preceding studies [27,28].

$$\mathrm{Hv} = 2F\frac{Sin68}{d^2} = 1.854\frac{F}{d^2} \ldots\ldots\ldots\ldots\ldots (14)$$

Where, d is the average diagonal length, H_V is the Vickers hardness, F is the indentation force or Load in gram of force (gf) and 1.854 is a constant of a geometric factor for the diamond pyramid. The calculated values of Al pure and Al-Lix (where x=1, 2, 3, 4 and 5 wt. %), melt–spun alloys are given in table.5.Can be see that the microhardness value increased from of pure aluminum as melt – spun ribbons and increased of Al-Lix at (x=1,2,3,4 wt.%) alloys .But then the microhardness values decreased of Al-2Li and Al-5Li wt.% alloys. can be interpreted this decrease of microhardness of Al-2Li and Al-5Li alloys to disturbance of structure as showed in the scanning electron microscopy. The rise in values hardness attributed to the effect of quantities lithium significantly. Note from hardness measurements there are effect significantly of the distribution of lithium particles which explain the behavior of the grain and particles size of the distribution of lithium particles in the alloys produced by melt–spun technique. Mahmudi et al [29] also, Romina [30] reported that there are three methods to calculated the exponent of stress (n),from indentation creep in the stable-state creep. Mustafa Kamal et al[31] were used most suitable method to examine indentation creep behavior of Al pure and Al-Lix (x=1,2,3,4 and 5 wt.%) alloys at room temperature by measuring the stress exponent of these alloys.

Table 5: the hardness and stress exponent melt spun alloys system.

Composition w.t% as melt spun Ribbons	Hardness Hv (MPa)	stress exponent (n)
Al pure	295.47	4.62
Al-1Li	359.66	1.36
Al-2Li	296.94	1.12
Al-3Li	370.44	2.89
Al-4Li	400.82	9.59
Al-5Li	293.02	2.93

The rate of diagonal difference is plot versus the Vickers hardness number on a double logarithmic scale as appeared in Fig. 6 for Al pure and Al-Li_x (where x=1, 2, 3, 4 and 5 wt. %) alloys. from straight line calculated stress exponent (n) to each alloys as show in table.5. It is shown that grain limits sliding is the conceivable technique amid room temperature Al-1Li, Al-2Li, Al-3Li and Al-5Li alloys. However, value exponent of stress (n= 9.6) may be associated with hardens during room temperature of Al-4Li alloys. According to the power law creep, an increase in stress exponent for Al-4Li would result in a decrease in creep rate due to an increase in yield strength[32]. Therefore, the value stress exponent higher (n) of Al-4Li alloy is more resistant to creep of indentation compared of Al-Lix (x=1, 2,3and 5) alloys.

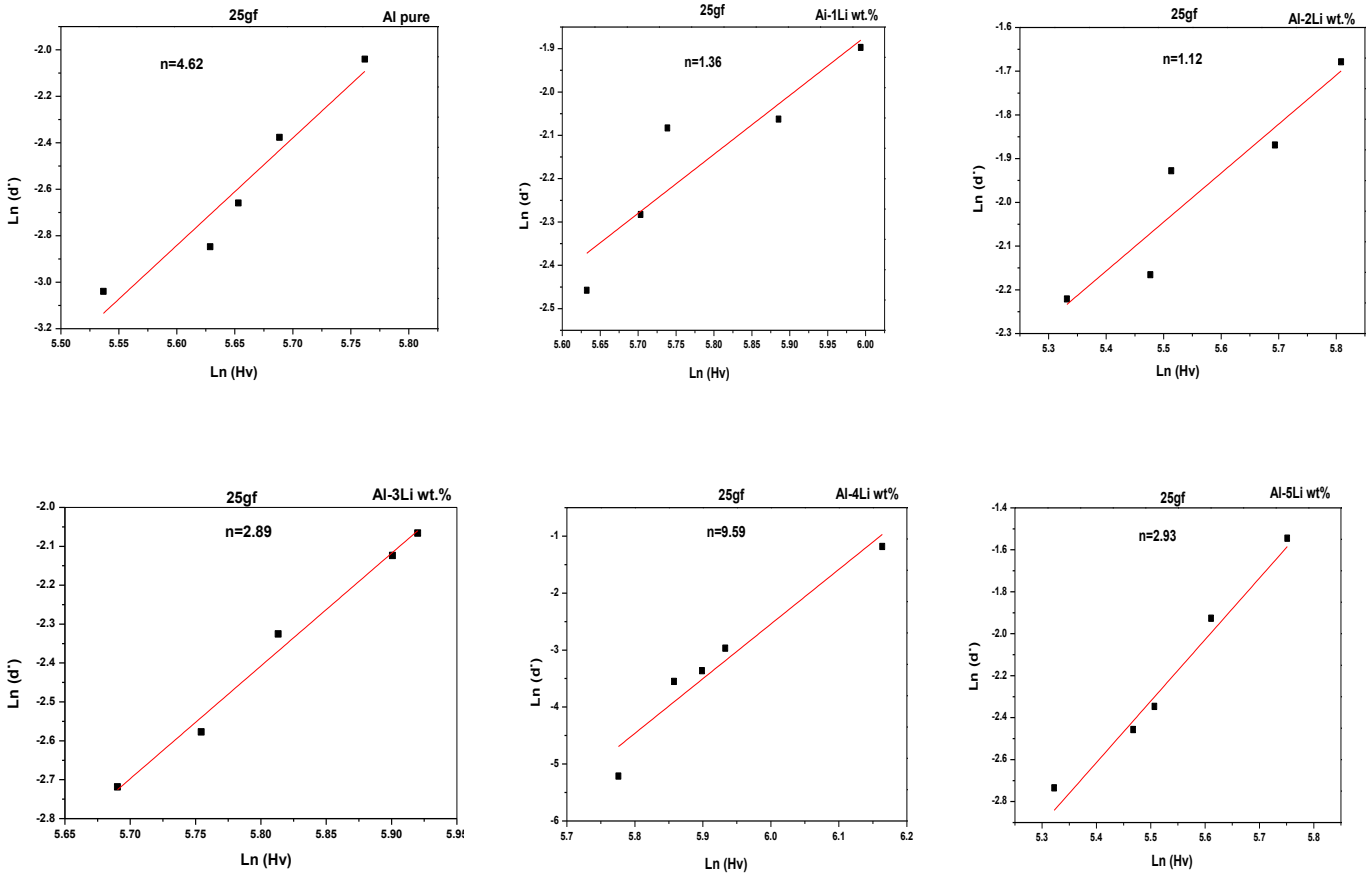

Fig.6: Indentation creep of melt spun alloys system.

6. Conclusion

There are changes in the mechanical, microstructure and Microhardness of the Al–Lix (where x=1234 and 5 wt. %) alloys were studied as following :

1. From examination of x-ray diffraction patterns show that the Al pure and Al–Lix (where x=1, 2, 3, 4 and 5 wt. %) alloys were composed of α-Al and Al8.9-Li1.1phases, each of them has the same orientation of growth.
2. Rapidly solidified process (RSP) significant effect on increasing the hardness, helped improvement of mechanical properties, attributed to decrease segregation of lithium, reduced the grain size and refinement of structural and the supersaturated solid solution.
3. Significant reductions in density, increase young modulus from lithium additions to aluminum alloys generate contribute increasingly broad application in aeronautics, as an alternative for the aluminum alloys.
4. Change lithium content to Aluminum alloys produced a change in microstructure (unit cell volume, lattice parameter and practical size), and the formed phases.
5. The mechanical data conclude that the lithium content has profound influence on the strength and stiffness of these rapidly solidified ribbons from melt.
6. From measurements thermal diffusivity there are a slightly variations of thermal diffusivity maybe due to segregation of Al8.9-Li1.1nanoparticles as indicated in the x-ray diffraction examination.
7. The value stress exponent higher (n) of Al-4Li alloy is more resistant to creep of indentation compared of Al-Lix (x=1, 2,3and 5wt. %) alloys.

7. References

[1] Y. Deng, J. Yang, S. Li, J. Zhang, X. Zhang, Influence of Li addition on mechanical property and aging precipitation behavior of Al-3.5Cu-1.5Mg alloy, Trans. Nonferrous Met. Soc. China. 24 (2014) 1653–1658.

[2] F.C. Campbell, Manufacturing Technology for Aerospace Structural Materials, Elsevier. (2006).

[3] H.-G. Li, J. Ling, Y.-W. Xu, Z.-G. Sun, H.-B. Liu, X.-W. Zheng, J. Tao, Effect of Aging Treatment on Precipitation Behavior and Mechanical Properties of a Novel Aluminum–Lithium Alloy, Acta Metall. Sin. (English Lett. 28 (2015) 671–677.

[4] F. Zhang, J. Shen, X.D. Yan, J.L. Sun, X.L. Sun, Y. Yang, Homogenization heat treatment of 2099 Al-Li alloy, Rare Met. 33 (2014) 28–36.

[5] B. Ahmed, S. Wu, Aluminum Lithium Alloys (Al-Li-Cu-X) -New Generation Material for Aerospace Applications, 440 (2014) 104–111.

[6] I.J. Polmear, M.J. Couper, Design and development of an experimental wrought aluminum alloy for use at elevated temperatures, Metall. Trans. A. 19 (1988) 1027–1035.

[7] N.E. Prasad, A. A. Gokhale, P.R. Rao, Mechanical behaviour of aluminium-lithium alloys, Sadhana. 28 (2003) 209–246.

[8] ASM INTERNATIONAL HANDBOOK COMMITTEE, et al. ASM Ha ndbook: Volume 3: Alloy Phase Diagrams. USA: The Materials Information Society , 1992, 200 .

[9] Fuller, Scott J. An Investigation of the As - Quenched and Early Aging Characteristics of a Al - 4.1 wt.% Li Binary Alloy by X - Ray Diffraction . NAVAL POSTGRADUATE SCHOOL MONTEREY CA, 1990 .

[10] J. Fragomeni, R. Wheeler, K. V Jata, Effect of Single and Duplex Aging on Precipitation Response , Microstructure , and Fatigue Crack Behavior in Al-Li-Cu Alloy AF / C-458, 14 (2005) 18–27.

[11] R.K. Gupta, N. Nayan, G. Nagasireesha, S.C. Sharma, Development and characterization of Al–Li alloys, Mater. Sci. Eng. A. 420 (2006) 228–234.

[12] R.J. Rioja, J. Liu, The Evolution of Al-Li Base Products for Aerospace and Space Applications, 43 (2012) 3325–3337.

[13] Y. Lin, Z. Zheng, S. Li, X. Kong, Y. Han, ScienceDirect Microstructures and properties of 2099 Al-Li alloy, Mater. Charact. 84 (2013) 88–99.

[14] E.J. Lavernia, N.I.C.H.O.L.A.S.J. Grant, Review Aluminium-lithium alloys, J. Mater. Sci. 22 (1987) 1521–1529.

[15] R.J. M. Kamal, J. c. Pieri, Memories et Etudes scientifiqes Revue de Metallurgie-Mars, (1983) 143–148.

[16] R. Cheese, B. Cantor, Superplasticity in splat-quenched Pb□Sn eutectic, Mater. Sci. Eng. 45 (1980) 83–93.

[17] H.H. Liebermann, The dependence of the Geometry of glassy alloy ribbons on the chill block melt-spinning process parameters, Mater. Sci. Eng. 43 (1980) 203–210.

[18] Rizk Mostafa Shalaby, Influence of indium addition on structure , mechanical , thermal and electrical properties of tin – antimony based metallic alloys quenched from melt, J. Alloys Compd, 480 (2009) 334–339.

[19] P. Duwez, R.H. Willens, W. Klement, Continuous Series of Metastable Solid Solutions in Silver-Copper Alloys, J. Appl. Phys. 31 (1960) 1136.

[20] S.U.N. Yi, Z. Mi-lin, H.A.N. Wei, L.I. Mei, Y. Yu-sheng, Electrochemical Formation of Al-Li Alloys by Codeposition of Al and Li from LiCl-KCl-AlF 3 Melts at 853 K, 29 (2013) 324–328.

[21] A.J. R. Manaila, F. Zavaliche, R. Popescu, D. Macovei, A. Devenyi, C. Bunescu, E. Vasile, No Title, Mater. Sci. Eng. A 226-228 (1997) 290–295.

[22] Rizk Mostafa Shalaby, M. Younus, Mustafa Kamal, Council for Innovative Research, ISSN 2347-348. 8 (2015).

[23] E.S. O. L. Anderson, and N, Soga, Elastic Constants and their Measurements, Soga, Elastic Constants Their Meas. (1973) 82–125.

[24] G. Roebben, B. Bollen, A. Brebels, J. Van Humbeeck, I. Introduction, Impulse excitation apparatus to measure resonant frequencies , elastic moduli , and internal friction at room and high temperature, (1997) 4511–4515.

[25] Mustafa Kamal, A.M. Shaban, M. El-Kady, R.M. Shalaby, Irradiation, mechanical and structural behaviour of Al-Zn-based alloys rapidly quenched from melt, Radiat. Eff. Defects Solids. 138 (1996) 307–318.

[26] J.J. Gilman, Mechanical behavior of metallic glasses, J. Appl. Phys. 46 (1975) 1625–1633.

[27] M. Yan, W.Z. Zhu, B. Cantor, The microstructure of as-melt spun Al – 7 % Si – 0 . 3 % Mg alloy and its variation in continuous heat treatment, Mater. Sci. Eng. A. 284 (2000) 77–83.

[28] O. Uzun, T. Karaaslan, M. Gogebakan, M. Keskin, Hardness and microstructural characteristics of rapidly solidified Al-8-16 wt.%Si alloys, J. Alloys Compd. 376 (2004) 149–157.

[29] R. Mahmudi, A. Rezaee-Bazzaz, H.R. Banaie-Fard, Investigation of stress exponent in the room-temperature creep of Sn-40Pb-2.5Sb solder alloy, J. Alloys Compd. 429 (2007) 192–197.

[30] R. Roumina, B. Raeisinia, R. Mahmudi, Room temperature indentation creep of cast Pb-Sb alloys, Scr. Mater. 51 (2004) 497–502.

[31] Mustafa Kamal, A.R. Lashin, Copper effects in mechanical properties of rapidly solidified Sn – Pb – Sb Babbitt bearing alloys, Mater. Sci. Eng. A. 530 (2011) 327–332.

[32] G. Cseh, J. Bär, H.J. Gudladt, J. Lendvai, A. Juhász, Indentation creep in a short fibre-reinforced metal matrix composite, Mater. Sci. Eng. A. 272 (1999) 145–151.